

Jan Klesa

Numerical stability of the intrinsic equations for beams in time domain

In: Jan Chleboun and Pavel Kůs and Petr Příkryl and Miroslav Rozložník and Karel Segeth and Jakub Šístek and Tomáš Vejchodský (eds.): Programs and Algorithms of Numerical Mathematics, Proceedings of Seminar. Hejnice, June 24-29, 2018. Institute of Mathematics CAS, Prague, 2019. pp. 71–80.

Persistent URL: <http://dml.cz/dmlcz/703064>

**Terms of use:**

© Institute of Mathematics CAS, 2019

Institute of Mathematics of the Czech Academy of Sciences provides access to digitized documents strictly for personal use. Each copy of any part of this document must contain these *Terms of use*.



This document has been digitized, optimized for electronic delivery and stamped with digital signature within the project *DML-CZ: The Czech Digital Mathematics Library*  
<http://dml.cz>

## NUMERICAL STABILITY OF THE INTRINSIC EQUATIONS FOR BEAMS IN TIME DOMAIN

Jan Klesa

Department of Aerospace Engineering, Faculty of Mechanical Engineering  
Czech Technical University  
Karlovo namesti 13, Prague, Czech Republic  
jan.klesa@fs.cvut.cz

**Abstract:** Intrinsic equations represent promising approach for the description of rotor blade dynamics. They are the system of non-linear partial differential equations. Stability of numeric solution by the finite difference method is described. The stability is studied for various numerical schemes with different methods for the computation of spatial derivatives from time level  $n + 0.5$  (i.e., mean values of old and new time step) to  $n + 1$  (i.e., only from new time step). Stable solution was obtained only for schemes between  $n + 0.55$  and  $n + 0.9$ . This does not correspond to the assumption that more implicit schemes have more numeric stability.

**Keywords:** finite difference method, intrinsic equations for beams, numeric stability

**MSC:** 65M06, 65M12

### 1. Introduction

Dynamics of beams represents very important branch in engineering praxis. Linear model is not sufficient for some types of problems, e.g. dynamics of some aircraft wings and helicopter rotor blades. Nonlinearity caused by big deflections must be considered in these cases. This led to the development of nonlinear beam models. One of them represented by intrinsic equations was presented by Hodges in [1] and [2]. It was later used in the field of beam dynamics. Finite element simulation of curved composite beams is presented in [3], Galerkin approach in [4]. Sotoudeh and Hodges used this model for the dynamics of helicopter blades in [5] and [6]. Using intrinsic equations has big potential for the improvement in the prediction of rotor blade dynamics. It leads to the solution of the non-linear partial differential equations. Numerical approach is chosen due to the complexity of the equations and often complicated blade geometry. Published results shows that there could exist problem with numerical stability, but there is no research work in this domain

known to the author. This paper tries to cover some basics aspects of this problem and describes numerical stability of intrinsic equations solved by the method of finite differences.

## 2. Methods

### 2.1. System of equations

System of nonlinear partial differential equations describes dynamics of beams with large displacement and small local deformation (linear elastic material model is used). It is based on the beam model presented in [2] and [5]. Each variable is vector with three components. Coordinate system is Cartesian.  $x_1$  axis is identical with beam axis,  $x_2$  and  $x_3$  axes defines beam cross section. Equations are derived for local coordinate system connected with beam centerline. This simplifies the equations. However, computation of displacement is more complicated (for details see [2] and [5]). System of differential equations consists of momentum conservation law (for both the linear momentum  $P$  and the angular momentum  $H$ ):

$$\frac{\partial P}{\partial t} = \frac{\partial F}{\partial x_1} + \tilde{K}F + f - \tilde{\Omega}P, \quad (1)$$

$$\frac{\partial H}{\partial t} = \frac{\partial M}{\partial x_1} + \tilde{K}M + (\tilde{e}_1 + \tilde{\gamma})F + m - \tilde{\Omega}H - \tilde{V}P. \quad (2)$$

Kinematic relations have to be added to the system:

$$\frac{\partial \gamma}{\partial t} = \frac{\partial V}{\partial x_1} + \tilde{K}V + (\tilde{e}_1 + \tilde{\gamma})\Omega, \quad (3)$$

$$\frac{\partial \kappa}{\partial t} = \frac{\partial \Omega}{\partial x_1} + \tilde{K}\Omega. \quad (4)$$

Nomenclature is described in Table 1.

Matrix  $\tilde{K}$  is defined by the elements of the vector  $K = [K_1 \ K_2 \ K_3]^T$  in following way (according to [2])

$$\tilde{K} = \begin{bmatrix} 0 & -K_3 & K_2 \\ K_3 & 0 & -K_1 \\ -K_2 & K_1 & 0 \end{bmatrix}. \quad (5)$$

Matrices  $\tilde{\Omega}$ ,  $\tilde{e}_1$ ,  $\tilde{\gamma}$  and  $\tilde{V}$  are defined in a similar way. Elements of vector  $K = [K_1 K_2 K_3]^T$  are actual beam twist  $K_1$ , actual beam curvature in  $x_2$  direction  $K_2$  and actual beam curvature in the  $x_3$  direction  $K_3$ . It consists undeformed beam twist and curvature  $k$  and elastic twist and curvature  $\kappa$

$$K = k + \kappa. \quad (6)$$

Constitutive relations close the system. It is assumed that beam elastic axis is identical with the axis  $x_1$  and the center of gravity of any cross-section is on the  $x_1$

$e_1$	Vector $[1 \ 0 \ 0]^T$
$f$	Vector of distributed applied force
$F$	Vector of internal force
$H$	Vector of cross-sectional angular momentum
$k$	Vector of undeformed beam curvature and twist
$K$	Vector of deformed beam curvature and twist
$m$	Vector of distributed applied moment
$M$	Vector of internal moment
$P$	Vector of cross-sectional linear momentum
$V$	Vector of velocity
$\gamma$	Vector of generalized strain
$\kappa$	Vector of elastic curvature and twist
$\Omega$	Vector of cross-sectional angular velocity

Table 1: Nomenclature.

axis. Then the transformation between beam elastic deformation  $\gamma$  and  $\kappa$  can be simplified to the form

$$\begin{Bmatrix} \gamma_{11} \\ 2\gamma_{12} \\ 2\gamma_{13} \\ \kappa_1 \\ \kappa_2 \\ \kappa_3 \end{Bmatrix} = \begin{bmatrix} \frac{1}{EA} & 0 & 0 & 0 & 0 & 0 \\ 0 & \frac{1}{GA_2} & 0 & 0 & 0 & 0 \\ 0 & 0 & \frac{1}{GA_3} & 0 & 0 & 0 \\ 0 & 0 & 0 & \frac{1}{GJ} & 0 & 0 \\ 0 & 0 & 0 & 0 & \frac{1}{EI_2} & 0 \\ 0 & 0 & 0 & 0 & 0 & \frac{1}{EI_3} \end{bmatrix} \begin{Bmatrix} F_1 \\ F_2 \\ F_3 \\ M_1 \\ M_2 \\ M_3 \end{Bmatrix}, \quad (7)$$

where  $EA$  is beam tensional stiffness,  $GA_2$  and  $GA_3$  are beam shear stiffnesses,  $GJ$  is torsional stiffness,  $EA_2$  and  $EA_3$  are beam bending stiffnesses. Relation between momentum and velocity (both linear and angular) can be written as

$$\begin{Bmatrix} P_1 \\ P_2 \\ P_3 \\ H_1 \\ H_2 \\ H_3 \end{Bmatrix} = \begin{bmatrix} \mu & 0 & 0 & 0 & 0 & 0 \\ 0 & \mu & 0 & 0 & 0 & 0 \\ 0 & 0 & \mu & 0 & 0 & 0 \\ 0 & 0 & 0 & i_2 + i_3 & 0 & 0 \\ 0 & 0 & 0 & 0 & i_2 & 0 \\ 0 & 0 & 0 & 0 & 0 & i_3 \end{bmatrix} \begin{Bmatrix} V_1 \\ V_2 \\ V_3 \\ \Omega_1 \\ \Omega_2 \\ \Omega_3 \end{Bmatrix}, \quad (8)$$

where  $\mu$  is beam mass per unit length,  $i_2$  and  $i_3$  are cross-sectional mass moments of inertia.

## 2.2. Boundary conditions

Usual boundary conditions for the simulation of blade or wing dynamics consists of 12 values, i.e., 4 vector variables. Internal force  $F$  and moment  $M$  equals to 0 at

the free end, i.e., wing or blade tip. Velocity  $V$  and angular velocity  $\Omega$  is defined at wing or blade root. This is the standard problem definition for blade dynamics. There is also possibility to simulate beam with both free ends (e.g. wing in flight). Force  $F$  and moment  $M$  equals then to zero at both wing (beam) ends. Wing movement is then the result of the simulation.

### 2.3. Initial values

Definition of initial values represents specific problem due to used set of variables. Velocity  $V$ , angular velocity  $\Omega$  and beam deformation  $\gamma$  and  $\kappa$  have to be defined for the whole beam. There are in fact two possibilities:

- Begin the simulation from the undeformed beam state, i.e.,  $\gamma = 0$  and  $\kappa = 0$ . This causes that transient process occurs during the first phase of the simulation in the time domain. This is not always acceptable.
- Begin the simulation from static (means time-independent in this case) solution. This requires extra step during which equations (1), (2), (3) and (4) are solved for  $\partial/\partial t = 0$ , i.e., as ordinary differential equations. This prevents transient process and give more precise results from the beginning of the simulation.

### 2.4. Computation of beam deflection

Price for the simplicity of intrinsic equations is missing node displacement  $u$  and node position  $r$  among equation variables. So displacement  $u$  have to be computed separately after the numerical solution of the equations (1) and (2). Node position vector of the deformed beam  $r + u$  can be computed by the means of following differential equation (according to [5]):

$$\frac{\partial(r + u)}{\partial x_1} = C^{iB}(e_1 + \gamma), \quad (9)$$

where  $r$  is position vector of given point on the beam centerline. Transformation matrix  $C^{iB}$  is the inversion of the matrix  $C^{Bi}$  which can be computed from the following equation

$$\frac{\partial C^{Bi}}{\partial x_1} = -(\tilde{k} + \tilde{\kappa})C^{iB}. \quad (10)$$

Beam deflection  $u$  is computed by numerical integration of (10) and (9) starting from the fixed end of the beam. Initial condition is represented by defined position of the first node (for studied case  $r = [0 \ 0 \ 0]^T$ , however,  $r \neq 0$  occurs in many technical applications).

## 3. Numerical solution

### 3.1. Discretization scheme

Finite difference method is used. Beam is divided to elements with equal length. More complex schemes can be applied in order to simulate changes of beam properties

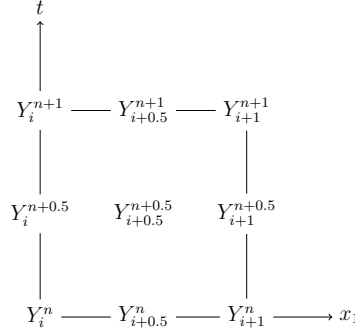


Figure 1: Schematic of time and space discretization at single beam element.

with  $x_1$ , bearings, complicated beam load etc.. Nodes are described by index  $i$ . System of equations is solved in the middle of each element, i.e., at point with index  $i+0.5$  (see Fig. 1). Scheme of the variables between the nodes  $i$  and  $i+1$  is presented in Fig. 1. Equations are computed in the middle of each element, i.e., in the points with spatial index  $i+0.5$ . Linear approximation is then used to obtain values in the nodes. The equations are solved in time domain by the means of finite difference method. Newton's method was used for the computation of the variables in the time step  $n+1$  from the values in the time step  $n$ . Code for the solution was written in the MATLAB environment.

### 3.2. Approximation of time derivatives

Standard forward discretization is used for the approximation of time derivatives

$$\begin{aligned} \frac{\partial y}{\partial t}(x_1 = X_{i+0.5}, t = T_{n+\theta}) &\approx \frac{Y_{i+0.5}^{n+1} - Y_{i+0.5}^n}{dt} = \\ &= \frac{0.5Y_i^{n+1} + 0.5Y_{i+1}^{n+1} - 0.5Y_i^n - 0.5Y_{i+1}^n}{dt}. \end{aligned} \quad (11)$$

### 3.3. Approximation of spatial derivatives

Central difference scheme is used so that approximation of spatial derivatives is computed in various time levels from  $n$  (i.e., explicit scheme) to  $n+1$  (i.e., standard fully implicit scheme). Explicit scheme was tested, but the computation was numerically unstable, so it was not used for detailed testing. So only implicit schemes were used. Spatial derivative is computed both from the values in time step  $n$  and  $n+1$ . E.g. designation  $n+0.6$  means that the approximation of the spatial derivative is computed from values  $Y^{n+\theta} = (1-\theta)Y^n + \theta Y^{n+1}$ . Formula for the approximation in the time level  $n+\theta$ , where  $\theta \in [0, 1]$ , is defined by

$$\begin{aligned} \frac{\partial y}{\partial x_1}(x_1 = X_{i+0.5}, t = T_{n+\theta}) &\approx \frac{Y_{i+1}^{n+\theta} - Y_i^{n+\theta}}{dx_1} = \\ &= \frac{\theta Y_{i+1}^{n+1} + (1-\theta)Y_{i+1}^n - \theta Y_i^{n+1} - (1-\theta)Y_i^n}{dx_1}. \end{aligned} \quad (12)$$

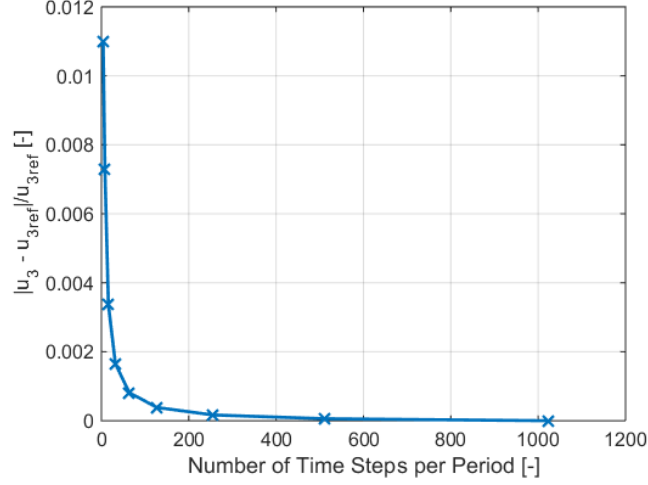


Figure 2: Relative error from the reference solution on the number of time steps per period, 60 elements, spatial derivatives computed at time level  $n+0.7$ .

### 3.4. Time step

All results presented in this paper were computed with the time step equal to  $1/64$  of period, i.e., time of one revolution. This is based on the comparison of the beam tip displacement with reference solution for various number of time steps per period (see Fig. 2). Reference solution has 1024 time steps per period.

### 3.5. Number of elements

All results presented in this paper were computed on 60 equally long elements on the beam, i.e., 61 nodes. This is based on the comparison of the beam tip displacement with reference solution for various number elements (see Fig. 3). Reference solution has 160 elements.

### 3.6. Problem definition

Simple rotating cantilever beam with harmonic loading in  $x_3$  direction is used for the testing of numerical stability. Beam characteristics were based on the test case from [5] and are presented in Table 2. Beam has no curvature and twist, i.e.,  $k = [0 \ 0 \ 0]^T$  for all elements.

Boundary conditions at the clamped end are defined by velocity  $V$  at the node  $i = 1$  equal to zero and angular velocity  $\Omega$  equal to  $[0 \ 0 \ \Omega_{ref}]^T$ . Boundary conditions at free end are defined at the last node by force  $F$  and moment  $M$  equal to zero. Beam is exposed to the harmonic load in the  $x_3$  direction equal to  $f_A(\cos(\Omega_{ref}t) - 1)$ . Value of  $f_A$  is  $10^4 N.m^{-1}$ .

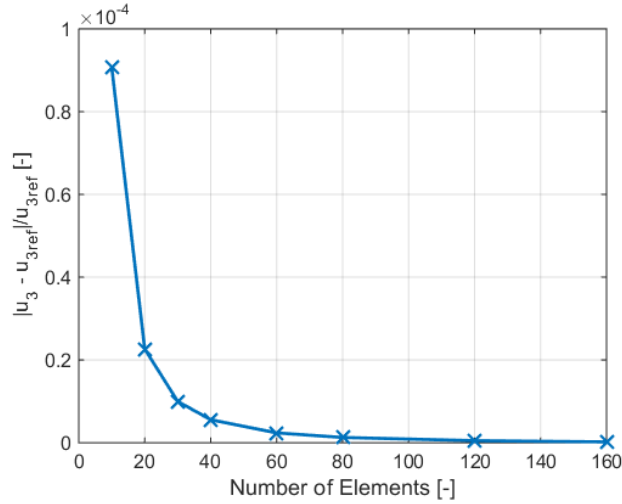


Figure 3: Relative error from the reference solution on the number of elements, 64 time steps per period, spatial derivatives computed at time level  $n+0.7$ .

Beam length	6	$m$
Mass per unit length $\mu$	35.72	$\text{kg.m}^{-1}$
Moment of inertia $i_2$	0.0005	$\text{kg.m}$
Moment of inertia $i_3$	0.0005	$\text{kg.m}$
Axial stiffness $EA$	$10^{10}$	$\text{N.m}^2$
Shear stiffness $GA_2$	$10^{10}$	$\text{N.m}^2$
Shear stiffness $GA_3$	$10^{10}$	$\text{N.m}^2$
Torsional stiffness $GJ$	$1.144 \times 10^6$	$\text{N.m}^2$
Bending stiffness (out of plane) $EI_2$	$1.132 \times 10^8$	$\text{N.m}^2$
Bending stiffness (inplane) $EI_2$	$1.436 \times 10^{10}$	$\text{N.m}^2$
Rotational velocity $\Omega_{ref}$	10	$\text{rad.s}^{-1}$
Number of elements	20	

Table 2: Beam data for the test case.

#### 4. Results

Results are presented in the form of computed dependence of beam tip deflection  $u_3$  on time. The correct solution corresponding to the beam with harmonic load is harmonic response in the form of beam tip deflection. Implicit schemes from  $n+0.45$  to  $n+1$  were tested. This included computation of spatial derivatives in time level  $n+0.5$ , i.e., method proposed by Hodges in [2] and used in [5].

System of intrinsic equations for beams shows very unusual characteristics. Numerically stable solution is obtained for the spatial derivatives computed in the time level  $n+0.7$ , see figure 4. This is used as reference solution for comparison. Stable

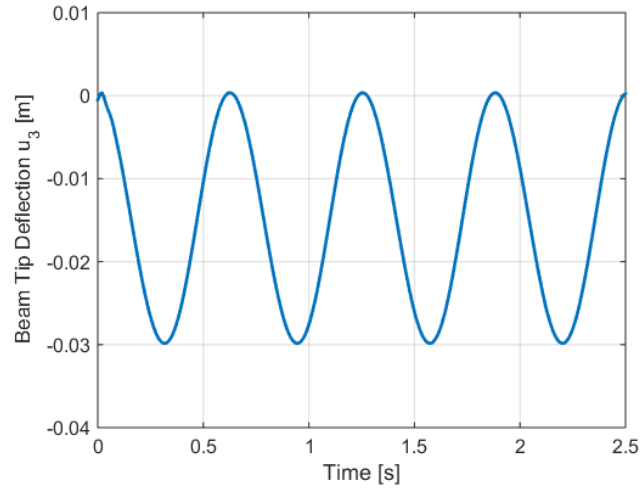


Figure 4: Stable solution with spatial derivatives computed at time level  $n+0.7$ .

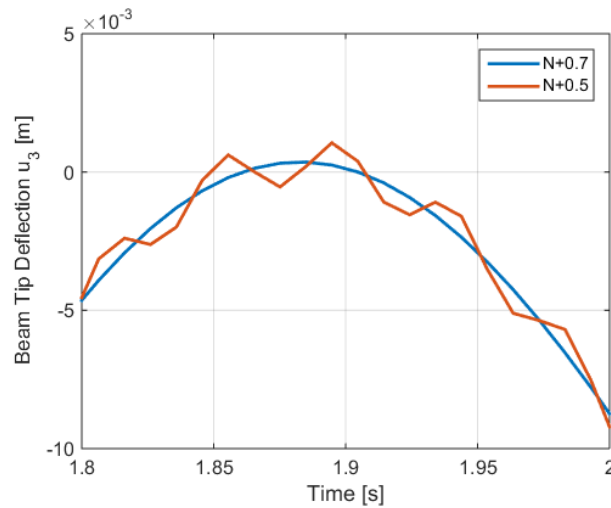


Figure 5: Demonstration of numerically induced oscillations for  $n+0.5$  in comparison with the stable solution for  $n+0.7$  (corresponds to the results published in [5]).

solution can be obtained for settings between approximately  $n + 0.55$  and  $n + 0.89$ . All settings from this interval gives numerically stable solution. If  $n + 0.5$  is used, non-physical numerically induced oscillations occur, see Fig. 5. This corresponds to the results presented in Fig. 15 in [5]. Further decrease of  $\theta$  leads to strong numerical instability as expected, see Fig. 6.

Increase of the value of  $\theta$  above 0.89 causes also numerical instability, see Fig. 7 for  $\theta = 0.9$ . This is quite surprising and unexpected phenomenon. Original expectation

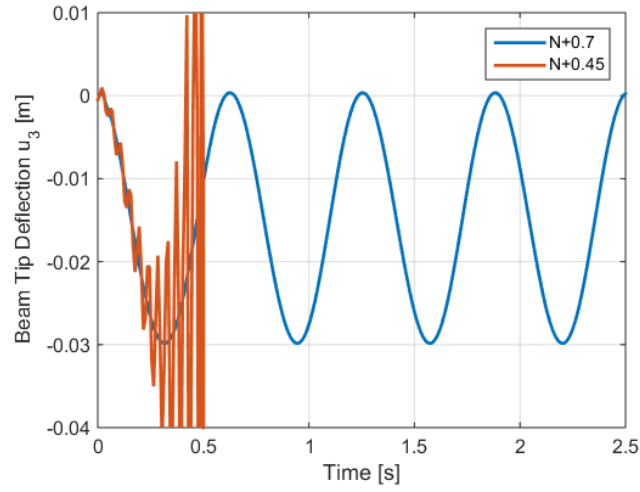


Figure 6: Unstable solution for  $n+0.45$ .

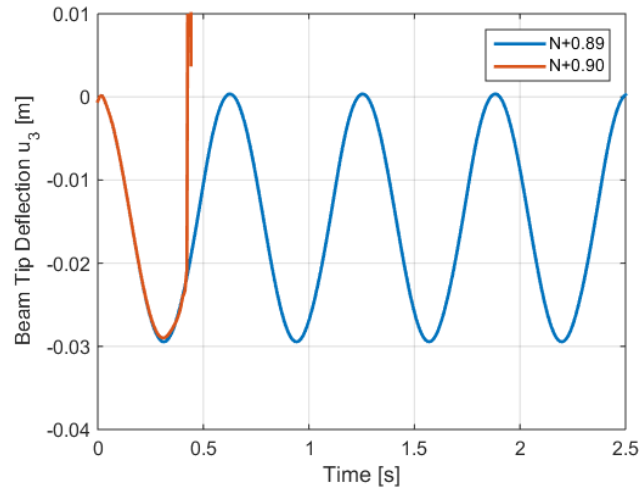


Figure 7: Unstable solution for  $n+0.9$ .

was that increase of the value of  $\theta$  brings more stable solution. However, this system of equations has interval of numerically stable solution for  $\theta$  approximately from 0.55 to 0.89. Some type of numeric instability can occur outside of this interval, e.g. numerically induced oscillations or divergence of the solution. Numerical stability for different number of elements were also tested with the conclusion that the stability region remains the same.

## 5. Discussion

Numerical stability of the solution of intrinsic equations for dynamics of beams is presented. Test case is simple cantilever rotating beam with harmonic load. Various discretization schemes are tested with the computation of spatial derivatives from the variables in different time levels  $n + \theta$  from  $n + 0.5$  to  $n + 1$ . The numerical solution is stable for the values of  $\theta$  between 0.55 and 0.89. Instability for lower values of  $\theta$  was expected and examples can be found in the literature.

Numerically unstable solution is obtained also for  $\theta$  higher than 0.9. Originally, it was assumed that higher value of  $\theta$  increases numerical stability of the solution. This assumption was not confirmed. Very surprising fact is that the solution is unstable for the fully implicit scheme, i.e., spatial derivatives are computed from the values in the next time step. Numerical stability does not depend on the number of beam elements. This information have to be respected during the development of numeric schemes for intrinsic equations.

## Acknowledgments

This work was supported by the EU Operational Program Research, Development and Education, under the Center of Advanced Aerospace Technologies, project No. CZ.02.1.01/0.0/0.0/16\_019/0000826.

## References

- [1] Hodges, D. H.: A Mixed Variational Formulation Based on Exact Intrinsic Equations for Dynamics of Moving Beams. *Int. J. Solids Structures*. **26** (1990), 1253–1273.
- [2] Hodges, D. H.: Geometrically Exact, Intrinsic Theory for Dynamics of Curved and Twisted Anisotropic Beams. *AIAA J.* **41** (2003), 1131–1137.
- [3] Hodges, D. H., Shang, X. and Cesnik, C. E. S.: Finite Element Solution of Non-linear Intrinsic Equations for Curved Composite Beams. *J. Am. Helicopter Soc.* **41** (1996), 313–321.
- [4] Patil, M. J. and Althoff, M.: Energy-consistent, Galerkin approach for the non-linear dynamics of beams using intrinsic equations. *J. Vib. Control*. **17** (2010), 1748–1758.
- [5] Sotoudeh, Z. and Hodges, D. H.: Structural Dynamics Analysis of Rotating Blades Using Fully Intrinsic Equations, Part I: Formulation and Verification of Single-Load-Path Configurations. *J. Am. Helicopter Soc.* **58** (2013), 032003.
- [6] Sotoudeh, Z. and Hodges, D. H.: Structural Dynamics Analysis of Rotating Blades Using Fully Intrinsic Equations, Part II: Dual-Load-Path Configurations. *J. Am. Helicopter Soc.* **58** (2013), 032004.